AIAA JOURNAL
Vol. 36, No. 6, June 1998

Controlling Unsteady Separation on a Cylinder with a Driven Flexible Wall

Dipankar Pal* and Sumon K. Sinha†
University of Mississippi, University, Mississippi 38677

A driven flexible wall consisting of an array of strip-shaped capacitive transducers is used to defer unsteady flow separation over a circular cylinder. The transducer elements, according to the need for detection and control of separation, are employed as wall pressure fluctuation sensors and vibrating-wall actuators. The spectrum of wall pressure fluctuations, sensed by a transducer element immediately upstream of the separation point, displays a dominant instability frequency. This frequency is believed to correspond to flow unsteadiness resulting from a passive interaction of the separating flow with the flexible wall. Actuation at this sensed frequency produces submicron-level vibration amplitudes of the wall normal to the boundary-layer flow. The mean separation point on the cylinder could be moved farther downstream by driving transducer elements slightly upstream of the sensing location. The control was effective at a frequency of 2.25 kHz for untripped and tripped boundary layers in the Reynolds number range from 1.2×10^5 to 1.5×10^5. This also reduced the mean pressure drag on the cylinder by 12 to 20%, reduced the size of the wake, and lowered velocity fluctuations inside the attached boundary layer and the separated shear layer.

Nomenclature

C_L = lift coefficient, $2L/(\rho U_\infty^2)$
C_p = pressure coefficient, $(p - p_\infty)/0.5\rho U_\infty^2$
d = diameter of cylinder
f = excitation frequency
H = height of wind-tunnel test section
h = vertical distance from cylinder midplane (upward positive)
L = lift force
l = length of cylinder
p = surface static pressure
p_∞ = upstream static pressure
Re_d = Reynolds number based on $d = (\rho U_\infty d)/\mu$
Sr_f = Strouhal number based on excitation frequency, fd/U_∞
T_i = freestream turbulence intensity, $(u^2 + v^2)^{0.5}/U_\infty$
U = mean streamwise velocity
U_∞ = upstream velocity
u = streamwise velocity fluctuation, rms
V = mean normal velocity
v = normal velocity fluctuation, rms
W = mean spanwise velocity
w = spanwise velocity fluctuation, rms
y = radial distance measured from cylinder surface
δ = boundary-layer thickness
θ = angular position from geometric forward stagnation point
μ = fluid dynamic viscosity
ρ = fluid density
$(')$ = velocities normalized with respect to U_∞

Introduction

CONTROLLING unsteady flow separation is of great importance in improving the performance of rotodynamic devices such as helicopter rotor blades and axial compressor blades. The localized interaction of wall vortices with the outer edge of the boundary-layer flow results in unsteady separation on such devices. The flow inside the attached boundary layer often goes through a cycle of forward and reversed velocities before breaking away from the wall. Attached unsteady boundary layers can be utilized to enhance the maximum lift that a wing or blade can generate. However, when the flow ultimately separates, the lift drops abruptly. Therefore, methods aimed at delaying the onset of breakaway separation of unsteady boundary layers are of practical interest. Unsteady effects are induced in these applications by the pitching or plunging motion of the lifting surface with respect to the approaching flow. Many important features of unsteady separating boundary layers over pitching or plunging lifting surfaces, e.g., the presence of near-wall reversed flow prior to separation, also are present in the boundary layer on a fixed circular cylinder in crossflow. Although significant differences exist between flows over cylinders and airfoils, controlling flow separation on a cylinder may be seen as the first step toward verifying the capability of a method.

The exact spatial location of the separation point and the exact instant of breakaway separation generally are not known a priori for unsteady separating flows. Hence, a system for efficient control of unsteady separation can be expected to incorporate an array of individually addressable wall actuators, e.g., wall suction, and sensors, e.g., microphones, within a feedback loop. Nelson et al.,[1] in their experimental study of boundary-layer transition control, demonstrated the effectiveness of such a sensor–actuator system in actively modifying the boundary-layer velocity profiles. Active devices, developed specifically for mitigating flow separation, range from oscillating flaps to jet vortex generators.[2] However, the mechanical complexity of these actuators and the additional need for sensors on the same surface often make them impractical for use on high-speed lifting devices and rotating components. The solution presented here is an array of transducers that can actively impart small-amplitude vibratory motion to a flexible wall. These transducers can be made extremely simple and robust without requiring the use of intricate actuation mechanisms. Additionally, the same transducers can serve as sensors, thereby simplifying the design even further.

Passive compliant walls have been known to interact with unstable waves over hydrodynamic surfaces.[3,4] By selecting the correct combination of wall stiffness and damping properties, along with the appropriate actuation parameters, i.e., forcing frequency, amplitude, and wavelength of small-scale surface waves, it should be possible to tailor the near-wall velocity profiles to achieve a desired control objective in liquid or gaseous flows. The objective may be drag reduction, transition delay, or separation control. However, the correct combination of wall properties and actuation parameters has remained rather elusive, especially for aerodynamic applications. In

Presented as Paper 97-0212 at the AIAA 35th Aerospace Sciences Meeting, Reno, NV, Jan. 6–9, 1997; received May 24, 1997; revision received Dec. 6, 1997; accepted for publication Jan. 10, 1998.

*Postdoctoral Researcher, Department of Civil Engineering. Member AIAA.
†Associate Professor, Department of Mechanical Engineering. Senior Member AIAA.

an experimental study by Weinstein,[5] drag reduction was negligible in a zero-pressure-gradient turbulent boundary layer perturbed by an array of acoustically driven flexible wall membranes. Bushnell et al.,[6] in their review paper, commented on the effectiveness of modulating the motion of passive compliant walls toward achieving drag reduction. The major problem identified by them was the unavailability of materials to construct walls having the requisite combination of mechanical properties to interact effectively with the boundary layer over a large range of flow conditions.

An actively driven flexible wall also can generate sound and interact with incident acoustic radiation. Experimental observations by Ahuja and Burrin[7] suggested the possibility of using incident acoustic radiation for deterring turbulent boundary-layer separation over airfoils. In the internal acoustic excitation experiments of Hsiao et al.,[8] sound waves were emanated through a narrow slot on the aerodynamic model to control unsteady and steady separating flows. Separated boundary layers on cylinders and airfoils could be reattached at subcritical Reynolds numbers by driving an acoustic speaker at appropriate frequencies. Lower sound pressure levels (SPL) were needed with this form of internal excitation compared with external excitation by speakers mounted on the wind-tunnel walls. Although acoustic radiation was assumed to be responsible for controlling the separation, subsequent experimental investigations by Williams et al.[9] suggested otherwise. An apparent lack of scaling with the SPL was observed, along with the fact that significant nonacoustic flow perturbation modes were generated by the acoustic sources used. This observation was verified later by the present authors,[10] who realized that flow-separation control was possible only if the perturbation velocities were three to four orders of magnitude higher than the acoustic particle velocities. This is needed to impart sufficient lateral momentum to alter the boundary-layer velocity profiles. As the flow Reynolds number increases, the effective perturbation frequencies also increase.[9,10] At higher frequencies, a larger fraction of the emanated power is consumed in increasing the SPL. Unless the total power output is increased, a point is reached when the speaker cannot produce velocity perturbations large enough to remain effective.

A driven flexible wall transducer therefore can be expected to interact mechanically with an attached boundary-layer flow, with acoustic interactions playing a secondary role. The overall interaction can be a combination of flow-induced wall oscillations along with motions produced by internal driving. This paper describes an experimental investigation of these interactions on a nominally two-dimensional oscillatory separating flow over a circular cylinder. The results of this proof-of-concept study provide a guideline for developing driven flexible-wall transducers for unsteady flow-separation control.

Experimental Arrangement

Flexible-Wall Transducer

The flexible-wall transducer[11] consists of an array of 1.6-mm-wide × 230-mm-long electrically conducting, strip-shaped elements. The strips are transversely mounted on the upper surface of the cylinder, as shown in Fig. 1. The gap between adjacent strips is 1.6 mm. A 6-μm-thick flexible polyester membrane covers the entire array of conducting strips. The membrane is aluminized on its outer face and has a mass density of 0.009 kg/m^2. The edges of the membrane are glued onto the cylinder surface such that there is adequate tension in the membrane to avoid large-scale surface roughness under flow conditions. The membrane is held down by electrostatic attraction of a 400-V dc bias applied across its metallized face and the conducting strips (Fig. 1). The strip-shaped elements form capacitive cells with the metallized face of the membrane. For each transducer element, a thin air gap exists between the bottom of the membrane and the conducting strip. The extent of this air gap under flow conditions defines the stiffness and damping properties of the flexible wall. The size of the air gap cannot be measured directly but has to be inferred from surface motion measurements.[12]

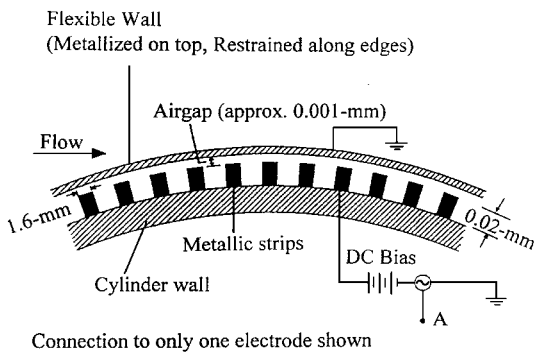

Fig. 1 Schematic of the array of flexible-wall transducers. Point A receives the sinusoidal driving voltage in the actuation mode and yields the wall pressure fluctuation signal in the sensor mode.

Each segment of the membrane above the conducting strips can be made to undergo flexural vibrations normal to the wall by superimposing a sinusoidal signal (20-V amplitude for this study) on the dc bias. Under no-flow conditions, the vibration amplitudes of the flexible wall are of the order of 10^{-4} mm, as inferred from laser Doppler vibrometer measurements.[12] For an excitation frequency range of 500 Hz to 20 kHz, the maximum surface velocity of the wall is about 5 mm/s. This is about four orders of magnitude lower than the freestream velocities of 12–30 m/s. The power needed to vibrate the flexible wall is of the order of a few microwatts. The laser Doppler vibrometer measurements also show the flexural vibrations to be localized, i.e., the wall motion produced by exciting a single strip damps out before reaching the adjacent strips.

Each strip-shaped capacitive cell of the transducer array also is designed to be used as a sensor for measuring flow fluctuations near the flexible wall. The output voltages, after the dc bias is isolated from the sensing elements, are dependent on changes in capacitance in the sensing cells. As long as the covering polyester membrane does not buckle under surface shear stress, changes in capacitance are produced solely on the basis of wall pressure fluctuations. Reducing the wall compliance by increasing the dc bias above 400 V suppresses high-frequency components greater than 5 kHz in the sensed signals and vice versa.

Wind-Tunnel Experiment

Experiments were conducted on a 152-mm-diam circular cylinder placed in crossflow in the 600 mm × 600 mm test section of a subsonic wind tunnel. The aspect ratio l/d and blockage ratio H/d were both 3.9. The flow Reynolds number Re_d was varied from 1.2×10^5 to 1.5×10^5 by varying the air speed. This range of Reynolds numbers corresponds to the transition from subcritical to critical flow over a rigid circular cylinder. The Strouhal number based on the vortex-shedding frequency remained practically constant at 0.21 at these Reynolds numbers.[13,14] The turbulence intensity T_i inside the test section was less than 0.3% for the entire range of flow velocities U_∞. The maximum flow Mach number, based on the streamwise velocity U at the edge of the boundary layer, ranged between 0.065 and 0.085. Therefore, the flow over the entire cylinder surface was considered to be incompressible except for the effects of small-amplitude acoustic radiation from the driven flexible wall. The array of flexible wall transducers was mounted on the upper surface of the cylinder so as to span the excursion of the separation point during a typical vortex shedding cycle. The membrane covered the angular region from $\theta = 65$ deg to $\theta = 100$ deg on the cylinder surface. To study the effect of wall actuation on a fully turbulent boundary layer as well, provision was made for placing a sandpaper trip, 80-grit size, transversely on the cylinder surface. The effective roughness height of the sandpaper was about 0.5 mm.

Instrumentation

A single-component hot-film probe (TSI Model 1210-60) and a single-component boundary-layer probe (TSI Model 1218-20) were used to measure the mean (U) and fluctuation (u) components of the streamwise velocity at various points: close to the flexible wall, in the separated shear layer, and inside the attached boundary layer. A two-component hot-film probe (TSI Model 1241-20) was used to measure mean (U and V) and fluctuation (u and v) components of streamwise and normal velocities inside the cylinder wake. This assumed that the mean and fluctuating components of the spanwise velocity (W and w) were significantly smaller than the other

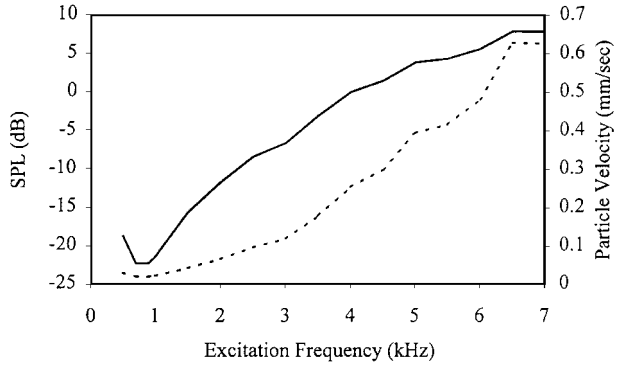

Fig. 2 Acoustic frequency response of a flexible-wall actuating element. SPL measurement and deduced acoustic particle velocities are at $y = 0.5$ mm from the flexible wall: ——, SPL, and - - - -, particle velocity.

two components (U, u and V, v). The hot-film measurements were replicable to within ±6 cm/s at 95% confidence level[15] for mean velocities between 1 and 35 m/s. The corresponding uncertainty level in the measurement of velocity fluctuations was ±1.5 cm/s in the measurement range of 0–5 m/s.

A differential pressure transducer (SETRA Model 264), communicating sequentially with surface-mounted static pressure taps, was used to detect changes in the time-averaged surface static pressures resulting from wall actuation. Static pressure taps were provided at 10-deg intervals over the entire circumference on the midsection of the cylinder. The time-averaged pressures had an uncertainty of ±1.43 Pa in 75 Pa within a 95% confidence level.[15] Time-averaged values of pressure-induced lift and drag forces on the cylinder were calculated by a numerical integration of the measured mean surface static pressures.

The SPL resulting from active wall vibration was measured with a 12.5-mm B&K condenser microphone. The SPL was measured in quiescent air at a distance of about 0.5 mm from the vibrating flexible surface. Because the acoustic wavelengths were at least an order of magnitude higher than 0.5 mm, small errors in this gap did not result in any appreciable errors in the measured SPL. The measured SPL was less than 10 dB (reference pressure = 0.1 Pa) in the excitation frequency range of 0.5–7 kHz. The SPL was not measured for the entire acoustic range because the microphone had only a flat frequency response, within ±0.5 dB, between 10 Hz and 7 kHz. Moreover, the frequencies of interest (see next section) were within this range. Acoustic particle velocities, computed from the measured SPL values, were less than 1 mm/s for this range of frequencies. The acoustic frequency response of a representative transducer element (in the midsection of the surface) is shown in Fig. 2. Comparison of excited strips near the edges and the central region of the transducer array showed less than a 5-dB difference in the corresponding SPL values. The variation in acoustic response along the length of each strip was within 7%.

Results

Optimum Frequency and Location for Actuation

In the present experiments, all results of flow separation control are reported at $Re_d = 1.5 \times 10^5$ because maximum effects could be observed at this Reynolds number. The excitation frequency f was chosen on the basis of the sensed wall pressure fluctuation spectrum near the mean separation point. Figure 3 shows the time-averaged spectrum of wall pressure fluctuations recorded by a sensor element at $\theta = 78$ deg, just upstream of the mean separation point,[14] in the absence of wall excitation. The broadband peak at 2.25 kHz seen in Fig. 3 is believed to indicate a flow-induced instability because the flexible-wall transducers did not have any mechanical or acoustic resonances at this frequency. Signals from other transducer strips in this region, i.e., 72 deg $< \theta <$ 80 deg, had higher background noise levels and did not show any clear peaks. This optimum excitation frequency corresponded to a Strouhal number Sr_f of about 23. This is an order of magnitude higher than Sr_f values reported for flow separation control with external and internal excitations using acoustic speakers.[7–10] To obtain the most effective location for wall excitation, the strips were excited one at a time and

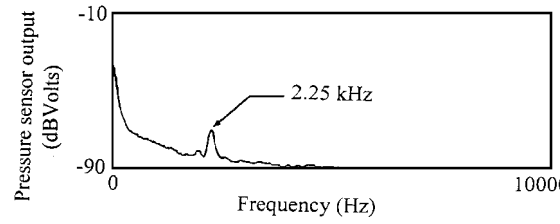

Fig. 3 Time-averaged surface pressure spectrum of the preseparation boundary layer in the absence of wall actuation ($Re_d = 1.5 \times 10^5$; measurement location $\theta = 78$ deg).

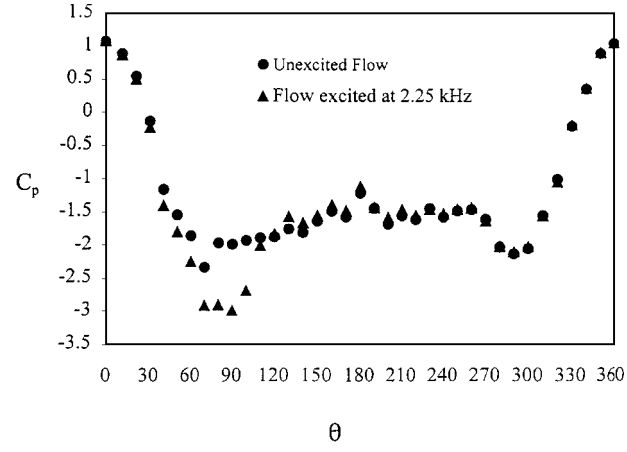

Fig. 4 Mean surface static pressure distribution for the untripped flow at $Re_d = 1.5 \times 10^5$ ($f = 2.25$ kHz, location of excitation $\theta = 72$–74 deg).

changes in mean surface static pressures were noted. Once the optimum angular location θ for the point of excitation was determined, the effect of driving multiple elements in phase was investigated. For $Re_d = 1.5 \times 10^5$, the largest changes in mean static pressures were observed when two adjacent strips, spanning the region between $\theta = 72$–74 deg, were excited in phase at $f = 2.25$ kHz. The efficacy of control, measured by changes in the time-averaged surface pressures, reduced with changing Reynolds number. Below $Re_d = 1.2 \times 10^5$, the changes in surface pressures due to wall excitation were smaller than the measurement uncertainty. Exciting individual strips between 72 and 74 deg also resulted in a smaller but measurable pressure change. Varying the excitation frequency more than ±0.25 kHz from the optimum value of 2.25 kHz also proved ineffective. Because of limitations in the maximum speed of the tunnel, the flow Reynolds number could not be increased beyond 1.5×10^5. Instead, the flow was tripped mechanically to investigate the effect of increasing the Reynolds number (see "Effect of Tripping").

Changes in Mean Lift and Drag

Figure 4 shows the changes in mean surface pressure coefficients C_p as a result of the wall excitation at 72 deg $\leq \theta \leq$ 74 deg and $f = 2.25$ kHz. A time-averaged lift coefficient C_L of 0.15 was estimated for the cylinder when no wall excitation was applied. The time-averaged C_L on a rigid circular cylinder should have been zero. The presence of the flexible wall on one side, i.e., only between 65 deg $< \theta <$ 100 deg, skewed the mean pressure distribution. This difference can be attributed to the passive compliance, damping, and small-scale roughness introduced by the flexible wall. Upon actuation at $f = 2.25$ kHz, for 72 deg $\leq \theta \leq$ 74 deg, the mean lift coefficient increased to 0.47 and the time-averaged pressure drag decreased by 12.4%.

Changes in Mean and Fluctuation Velocities

Figure 5a shows the time-averaged spectra of resultant velocity fluctuations, i.e., $(u^2 + v^2)^{1/2}$, measured with the single-component hot-film probe in the unexcited and excited boundary layers at $\theta =$ 74 deg and $y = 2$ mm. This measurement location corresponds to the preseparation boundary layer even under unexcited conditions.

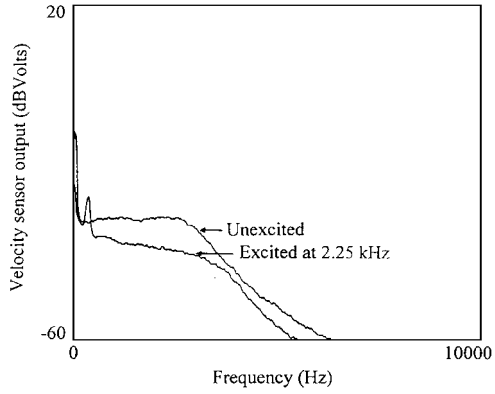

a) Preseparation: hot-film anemometer output shown at $\theta = 72$ deg, $y = 2$ mm

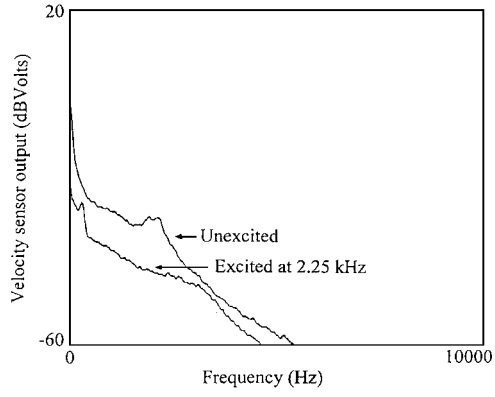

b) Postseparation: hot-film anemometer output shown at $\theta = 82$ deg, $y = 8$ mm

Fig. 5 Time-averaged velocity spectra of preseparation boundary layer and postseparation shear layer ($Re_d = 1.5 \times 10^5$, $f = 2.25$ kHz, excitation location $\theta = 72$–74 deg).

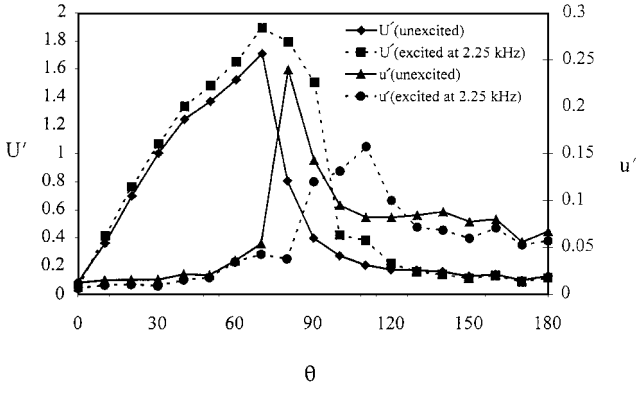

Fig. 6 Distribution of time-averaged mean and fluctuation velocities close to the cylinder surface ($y = 1$ mm for all measurement locations, $Re_d = 1.5 \times 10^5$, $f = 2.25$ kHz, excitation location $\theta = 72$–74 deg).

The ordinate of Fig. 5a shows the velocity-sensor output in decibel-volts and provides a comparison between velocity fluctuation magnitudes under unexcited and excited conditions. Figure 5b shows the same at a location where the unexcited boundary layer has already separated from the surface ($\theta = 82$ deg). In this case, the measurement was recorded at $y = 8$ mm because the measured velocity fluctuation levels maximized at that location. The unexcited spectrum shows a broad peak around 2.25 kHz, which is seen to disappear upon excitation.

Figure 6 shows the effect of excitation on the distribution of mean and fluctuation velocities at $y = 1$ mm. The separation point can be identified by an increase in velocity fluctuations denoted as u' and a corresponding decrease in the time-averaged streamwise velocities denoted as U'. Excitation is seen to move the mean separation point from $\theta \approx 80$ deg to $\theta \approx 100$ deg. For clarity, the data points in Fig. 6 have been joined by line segments. The largest value of velocity fluctuations is seen to reduce upon excitation. Also, the location of this maximum is observed to move back to $\theta = 110$ deg from $\theta = 80$ deg as a result of delayed separation. Finally, the time-averaged velocities (U') are found to increase both upstream and downstream of the region of excitation.

Two-component wake velocity measurements $1.5d$ behind the cylinder (Fig. 7a) showed that both U' and V' increased as a result of driving the wall. This indicated a change in the direction of the mean flow. Figure 7b indicates that the streamwise velocity fluctuations u' decreased in the wake, whereas the normal component v' of fluctuations increased in the center but decreased at the edges of the wake. In Figs. 7a and 7b, cross-stream coordinates h measured from the horizontal midplane of the cylinder have been normalized with respect to the cylinder radius $d/2$ and expressed as the normalized wake height $2h/d$. These results suggest that the size of the wake region diminished and the flow unsteadiness due to vortex shedding was reduced under wall excitation. The large asymmetry in mean velocities between the top and bottom halves of the wake is due to the asymmetric location of the flexible wall.

Effect of Tripping

Because the flow Reynolds numbers at which the effect of flexible-wall perturbation was studied were very close to the transitional Reynolds number for the cylinder, it was suspected that the forcing actually promoted the laminar-turbulent transition process. To study the effect of wall actuation on a fully turbulent boundary layer, the flow over the cylinder at $Re_d = 1.5 \times 10^5$ was tripped at $\theta = 35$ deg using the sandpaper trip. Single-element hot-film probe measurements showed large increases in the streamwise velocity fluctuations u, thereby indicating an increase in turbulence levels inside the boundary layer. The optimum region of wall excitation and the optimum driving frequency for separation control were found to remain unchanged. However, significant differences were observed (Fig. 8) in the distributions of time-averaged static pressures around the cylinder, under both unexcited and excited conditions. Compared to the untripped flow case of Fig. 4, the unexcited tripped flow showed better pressure recovery between 60 deg $< \theta <$ 120 deg. Wall excitation primarily increased the time-averaged static pressures in the wake of the cylinder (95 deg $< \theta <$ 300 deg). Numerical integration of the pressure distributions of Fig. 8 showed that exciting the tripped flow increased the value of C_L from 0.33 to 0.54, whereas the time-averaged pressure drag dropped by 20.2%.

Discussion

An array of flexible-wall transducers has been used to control unsteady flow separation on a circular cylinder. The transducer elements were first used as wall pressure fluctuation sensors. In this mode, a dominant instability frequency could be detected immediately upstream of the mean separation point. Flow separation could be deferred when a segment of the flexible wall, slightly upstream of the sensing location, was actively vibrated at the sensed frequency. The achievable degree of separation control depends on the interaction of the flexible wall with the flow. The properties of the active perturbation, e.g., amplitude, frequency, and location on the flexible surface; the structure of the flow; and the possible modes of energy transfer determine the effectiveness of this interaction.

Surface vibration amplitudes of the flexible wall could be correlated to the SPL generated as a result of active, i.e., non-flow-induced, wall excitation under quiescent conditions. For the present experiments, no changes were observed when the emanated SPL was less than −20 dB. Also, significantly higher SPL values, e.g., 40 dB, did not produce noticeable improvement. The acoustic wavelength in air at the optimum excitation frequency of 2.25 kHz was about 145 mm. This was not close to any of the known resonant modes in the wind tunnel. Hence, the acoustic component of the disturbances primarily perturbed the freestream flow above the boundary layer. Additionally, inside the boundary layer, the acoustic energy radiated by the vibrating wall was about two orders of magnitude lower than its vibrational kinetic energy.

The experiments showed that the present method of separation control is effective for a narrow range of Reynolds numbers and

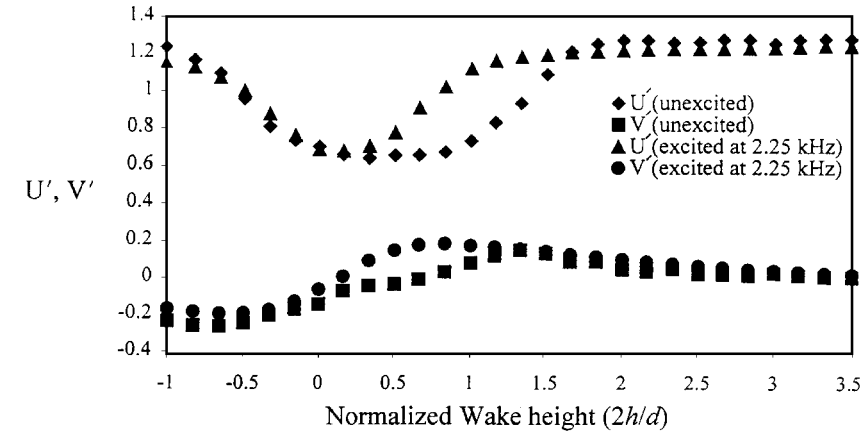

a) Mean velocities

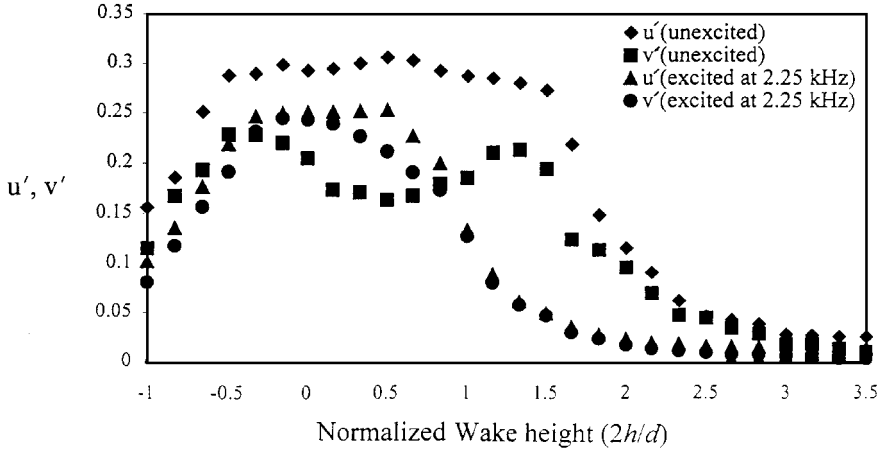

b) Fluctuation velocities

Fig. 7 Distribution of time-averaged streamwise and normal components of velocities in the cylinder wake (measurement location, 1.5*d* downstream of cylinder center; $Re_d = 1.5 \times 10^5$; $f = 2.25$ kHz).

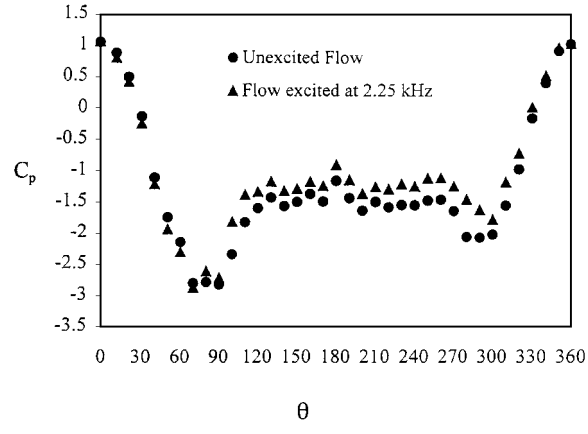

Fig. 8 Mean surface static pressure distribution during unexcited and excited flow states for the tripped flow at $Re_d = 1.5 \times 10^5$ ($f = 2.25$ kHz, flow tripped at $\theta = 35$ deg, location of excitation $\theta = 72$–74 deg).

excitation frequencies. This indicates that the method works only if conditions are favorable for small-amplitude wall perturbations ($\approx 10^{-4}\delta$) to grow inside the attached boundary layer. The velocity profile of the near-separation attached boundary layer on a cylinder has sharp gradients and points of inflection. The disturbances introduced by vibrating the wall probably lock onto the most amplified instability mode of the attached boundary layer. The presence of such receptive modes of flow instabilities explains the detection of the broadband frequency peak (Fig. 3) by a sensor element. Therefore, the location for driving the wall becomes extremely critical.

Conclusions

The present proof-of-concept experiments on unsteady flow separation control revealed the following.

1) The sensed instability frequency was the most effective frequency for separation control. The Strouhal number Sr_f based on this frequency was about 23.

2) The control was effective for near-critical laminar flow and tripped turbulent flow on the cylinder at $1.2 \times 10^5 \leq Re_d \leq 1.5 \times 10^5$. The corresponding reductions in pressure drag due to delayed flow separation were 12.4% and 20.2%, respectively.

3) Extremely small-amplitude wall vibrations, $\mathcal{O}(10^{-4}\delta)$, were needed for effective separation control. The power input to the transducer was about 10^{-6} times the savings in power resulting from drag reduction.

4) The driven flexible wall appears to be exploiting some form of flow instability in the unsteady separating boundary layer. The acoustic wavelength at the control frequency of 2.25 kHz was significantly larger than the maximum boundary-layer thickness ($\approx$2 mm). Therefore, a nonacoustic mode of wall-flow interaction appears most likely.

5) In many ways, the effect of the single-frequency wall actuation on the near-separation flow looks similar to that of a tripped boundary layer. However, unlike the promotion of turbulence with a boundary-layer tripping device, driving the flexible wall reduced the resultant velocity fluctuations near the surface at practically all frequencies and almost all spatial locations upstream and downstream of the separation point.

Acknowledgments

This research was initiated through support from the Air Force Office of Scientific Research (Grant No. AFOSR 91-0410), under

the mentorship of Daniel Fant. The continuation work has been partially funded by Grants No. DAAH-04-93-G-0451 and DAAH-04-94-G-0268 from the Army Research Office under the mentorship of Thomas Doligalski. The authors gratefully acknowledge this support.

References

[1]Nelson, P. A., Rioual, J. L., and Fisher, M. J., "Experiments on the Active Control of Transitional Boundary Layers," *Proceedings of the Second International Congress on Recent Developments in Air and Structure Borne Sound and Vibration*, Auburn Univ., Auburn, AL, 1992, pp. 305–312.

[2]Gad-el-Hak, M., and Bushnell, D. M., "Separation Control: Review," *Journal of Fluids Engineering*, Vol. 113, No. 1, 1991, pp. 5–30.

[3]Carpenter, P. W., and Garrad, A. D., "The Hydrodynamic Stability of Flow over Kramer-type Compliant Surfaces, Part 1: Tollmien-Schlichting Instabilities," *Journal of Fluid Mechanics*, Vol. 155, June 1985, pp. 465–510.

[4]Carpenter, P. W., and Garrad, A. D., "The Hydrodynamic Stability of Flow over Kramer-Type Compliant Surfaces, Part 2: Flow-Induced Surface Instabilities," *Journal of Fluid Mechanics*, Vol. 170, Sept. 1986, pp. 199–232.

[5]Weinstein, L. M., "Effect of Driven Wall Motion on a Turbulent Boundary Layer," *Proceedings of the IUTAM Symposium on Unsteady Turbulent Shear Flows*, Springer–Verlag, 1981, pp. 58–66.

[6]Bushnell, D. M., Hefner, J. N., and Ash, R. L., "Effect of Compliant Wall Motion on Turbulent Boundary Layers," *Physics of Fluids*, Vol. 120, No. 10, Pt. 2, 1977, pp. S31–S48.

[7]Ahuja, K. K., and Burrin, R. H., "Control of Flow Separation by Sound," AIAA Paper 84-2298, Oct. 1984.

[8]Hsiao, F. B., Liu, C. F., and Shyu, J. Y., "Control of Wall Separated Flow by Internal Acoustic Excitation," *AIAA Journal*, Vol. 28, No. 8, 1990, pp. 1440–1446.

[9]Williams, D., Acharya, M., Bernhardt, J., and Yang, P., "The Mechanism of Flow Control on a Cylinder with the Unsteady Bleed Technique," AIAA Paper 91-0039, Jan. 1991.

[10]Sinha, S., and Pal, D., "On the Differences Between the Effect of Acoustic Perturbation and Unsteady Bleed in Controlling Flow Separation over a Cylinder," Society of Automotive Engineers, SAE Aerotech '93, TP 932573, Costa Mesa, CA, Sept. 1993.

[11]Sinha, S. K., "The ACOUSTOSURF—A Multi-Element Acoustic Active Surface for Flow Separation Control," U.S. Provisional Patent Application 60/030,489, Nov. 1996.

[12]Pal, D., "Mechanisms for Energy Transfer Between an Acoustically Active Compliant Wall and a Separating Boundary Layer," Ph.D. Dissertation, Dept. of Mechanical Engineering, Univ. of Mississippi, University, MS, May 1997.

[13]Farrel, C., and Blessman, J., "On Critical Flow Around Smooth Circular Cylinders," *Journal of Fluid Mechanics*, Vol. 136, Nov. 1983, pp. 375–391.

[14]Schlichting, H., *Boundary Layer Theory*, 4th ed., McGraw–Hill, New York, 1968, Chaps. 2 and 12.

[15]Coleman, H. W., and Steele, W. G., *Experimentation and Uncertainty Analysis for Engineers*, Wiley, New York, 1989, Chap. 3.

P. R. Bandyopadhyay
Associate Editor